Heliyon 9 (2023) e20136

Contents lists available at ScienceDirect

Heliyon

journal homepage: www.cell.com/heliyon

Short-pulsed Q-switched fiber laser using graphene oxide quantum dots based as saturable absorber

P. Zaca-Morán [a,*], Celia L. Gomez [a], O. Zaca Morán [b], J.G. Ortega-Mendoza [c], E.S. Pola-López [d]

[a] *Instituto de Ciencias, Benemérita Universidad Autónoma de Puebla, CP 72050, Puebla, Mexico*
[b] *Instituto Politécnico Nacional, Centro de Investigación en Biotecnología Aplicada, Ex–Hacienda de San Juan Molino, Km 1.5 de la Carretera Estatal Santa Inés Tecuexcomac-Tepetitla, Tepetitla, CP 90700, Tlaxcala, Mexico*
[c] *División de Posgrado, Universidad Politécnica de Tulancingo, Tulancingo de Bravo, Hidalgo, CP 43629, Mexico*
[d] *Tecnológico Nacional de México, Instituto Tecnológico de Tuxtla Gutiérrez, Maestría en Ciencias en Ingeniería Mecatrónica, CP 29050, Tuxtla Gutiérrez, Chiapas, Mexico*

ARTICLE INFO

Keywords:
Graphene oxide
Quantum dots
Optical fibers
Nonlinear characterization
Nonlinear susceptibility

ABSTRACT

In this work, we report the experimental study of a Q-switched optical fiber laser based on graphene oxide quantum dots (GOQDs) as saturable absorber (SA). GOQDs are fabricated by carbonization and exfoliation electrospun polyacrylonitrile (PAN) fibers. The results of Fourier Transform Infrared Spectroscopy (FTIR) showed bands caused by the CHs and C═O groups associated with the GOQDs. The Raman spectrum showed the typical G and D bands of GOQDs. The size of the GOQDs, calculated by Transmission Electron Microscopy (TEM) was 6 nm; additionally, by high resolution TEM (HRTEM), an interplanar distance of 0.19 nm corresponding to the (002) direction of the graphene oxide was calculated. The SA was achieved using the photodeposition technique of the GOQDs onto the core of a single-mode optical fiber. The nonlinear characterization (NLC) of the GOQDs was carried out using the P-scan technique with a high-gain erbium-doped fiber amplifier (EDFA) at a wavelength of 1550 nm. The obtained results showed a saturable absorption behavior with a value of $\beta = -1.178\,x10^{-6}\ (m/W)$ and a nonlinear susceptibility of $Im(\chi^{(3)}) \approx -1.573x10^{-7}\ (esu)$. The experimental results of the SA, based on GOQDs as a switching device in a fiber laser, showed a typical behavior of a Q-switched laser by generating a pulsed emission at a wavelength of 1599 nm, a frequency from 2 to 16 kHz, and a maximum average output power of 1.3 mW.

1. Introduction

Nanomaterial-based passive switching devices have contributed significantly in the field of optics by generating short and ultrashort pulses in optical fiber lasers [1]. Many of these switching devices, commonly known as saturable absorbers (SAs), are carbon-based materials such as nanotubes [2–4], graphene [5–9], and graphene oxide [10–16]. So far, the most commonly used techniques for the implementation of these SAs have been dip or drip deposition [3,10,11], thin films or membranes [4–7,12,13,15,16] and photodeposition [9,14].

* Corresponding author.
E-mail address: placido.zaca@correo.buap.mx (P. Zaca-Morán).

https://doi.org/10.1016/j.heliyon.2023.e20136
Received 31 August 2023; Received in revised form 10 September 2023; Accepted 12 September 2023
Available online 13 September 2023

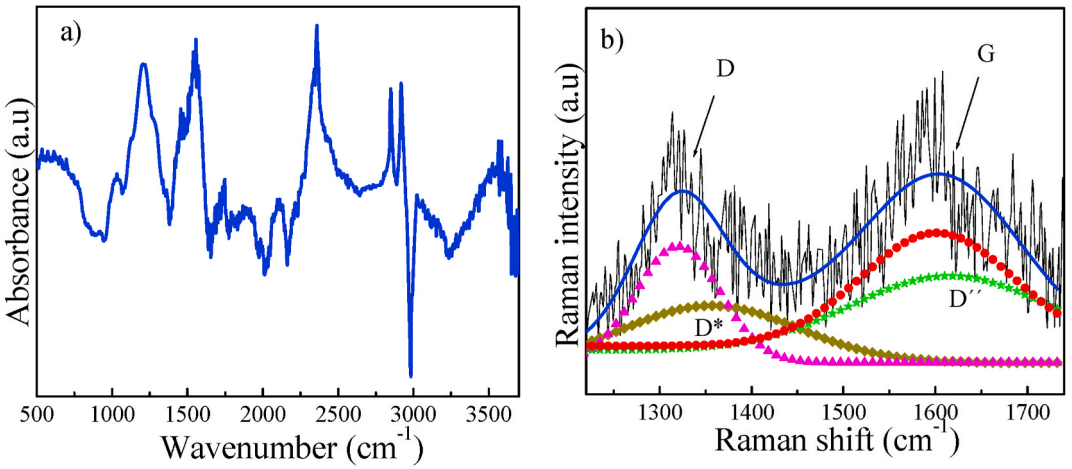

Fig. 1. a) FTIR and b) Raman spectra of carbonized PAN fibers at 1100 °C.

Yap Y. et al. [14] recently reported a study about the optical deposition of reduced graphene oxide (rGO) on the cross-section of an optical fiber for implementation as a SA device in a ring cavity laser. Their results showed the generation of pulses with a repetition frequency of ~85 kHz and pulse durations of ~2 μs with emission at 1533 nm. On the other hand, Yap Y–K. et al. [17] reported a SA for a Q-switch laser using graphene oxide flakes, the SA was performed sandwiching a film between two fiber adapters. The results obtained in a ring cavity laser showed pulsed emission at 1563 nm with a frequency of 21.5 kHz and a temporal width of 3.78 μs Additionally, Liu S. et al. [18] reported the presence of saturable absorption of two photons at 1000 nm using graphene quantum dots obtained by the solvothermal method. The SA was implemented using a solution-coated mirror with graphene quantum dots. Their results showed a pulsed emission of 1.13 MHz at 1063.03 nm of wavelength using a semiconductor laser. Recently, low-dimensional materials, such as carbon-based quantum dots, have been of great interest in the field of nonlinear optics and their applications as switching devices in pulsed fiber lasers [19–23]. However, Q-switched lasers based on GOQDs photodeposited on an optical fiber have not been explored yet.

In this work, the experimental setup of a Q-switched fiber laser based on GOQDs, obtained from carbonized and exfoliated PAN electrospun fibers, is reported. The structural and morphological characterization of the GOQDs, as well as the non-linear susceptibility of the saturable absorption device are included. The NLC of the GOQDs was measured using the P-scan technique by an EDFA with emission at 1550 nm. The results obtained showed that GOQDs can be used in a Q-switched fiber laser.

2. Fabrication of GOQDS and Q-switched fiber laser setup

2.1. Fabrication of GOQDs

GOQDs were obtained from the carbonization and exfoliation of electrospun PAN fibers [24]. A solution of PAN diluted to 10% by weight in N–N-Dimethylformamide (DMF) was prepared, keeping it under agitation for 12 h at room temperature. The fibers were fabricated by introducing the polymeric solution into an electrospinning system (Spellma High Voltage DC Supply) using 15 kV and a collection time of 10 min at room temperature. The fibers obtained were thermally treated at 270 °C for 30 min under atmospheric conditions with a heating ramp of 5 °C/min to stabilize them structurally. Subsequently, the fibers were carbonized at 1100 °C in a nitrogen atmosphere, with a heating ramp of 5 °C/min to obtain graphite oxide. Finally, the graphite oxide fibers were mixed with isopropyl alcohol (C3H8O, Sigma Aldrich) and exfoliated in an ultrasonic bath (Branson 3800) at 40 kHz for 90 min.

2.2. Morphological and structural characterization of PAN fibers and GOQDs

The carbonized fibers and the GOQDs were characterized by FTIR spectroscopy in the region of 4000 to 400 cm-1 by a spectrophotometer (Bruker Vertex 70) in attenuated total reflection (ATR) mode. Raman spectra of carbonized fibers and GOQDs were obtained with a spectrophotometer (Thermo Scientific DXR Smart Raman) in an operating range of 50–3350 cm-1 with an excitation laser of 780 nm with 12 mW output power and a thermoelectrically cooled CCD detector. The morphology of the GOQDs was studied with a TEM (Tecnai G2 T20) operated at 300 kV. Morphological studies of HRTEM (TESCA JEOL JEM200) using an operating voltage of 80–200 kV were performed using Gatan Digital Micrograph software.

The FTIR spectroscopy results of the PAN fibers (Fig. 1a) show signals in the region from 2924 to 2870 cm^{-1} related to the CH functional groups; also, between 1386 and 1640 cm^{-1} associated with C═C stretching vibrations in the aromatic ring, and C–H bending mode. In addition, the associated signal with C–O bond stretching mode which is coupling at 1190 cm^{-1} [25]. While the Raman spectrum (Fig. 1b) shows two main bands, one at 1320 cm^{-1}, known as the D band, which is associated with the presence of defects or disorder in the lattice, and another one at 1595 cm^{-1} assigned as G band, both of which correspond to graphite [26]. The

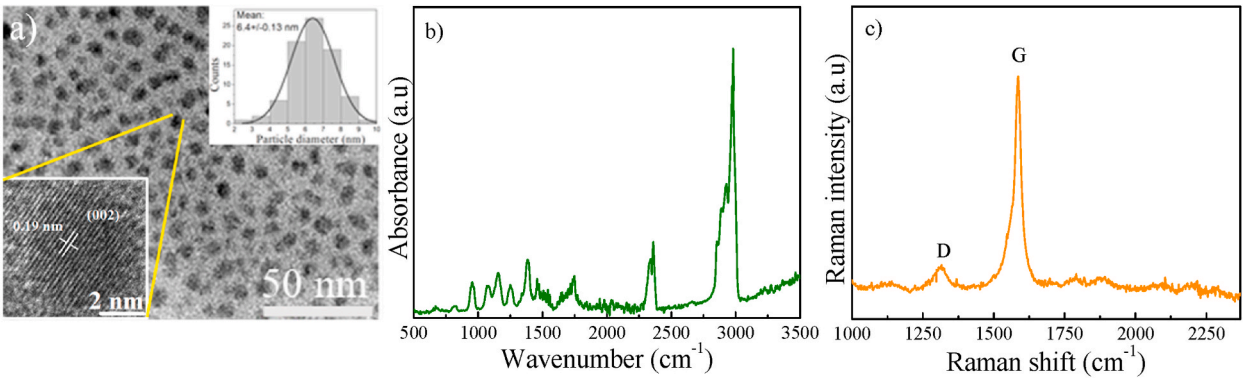

Fig. 2. a) TEM micrograph of the GOQDs. Insets (top: size distribution histogram, and bottom: HRTEM micrograph of a GOQD), b) FTIR spectrum of the GOQDs, and c) Raman spectrum of the GOQDs.

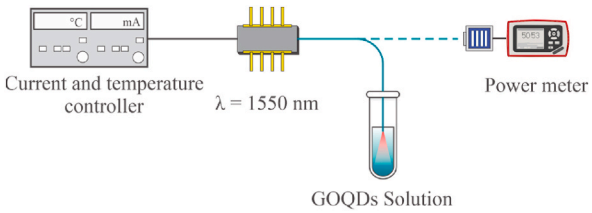

Fig. 3. Experimental setup for the photodeposition of GOQDs onto optical fiber end.

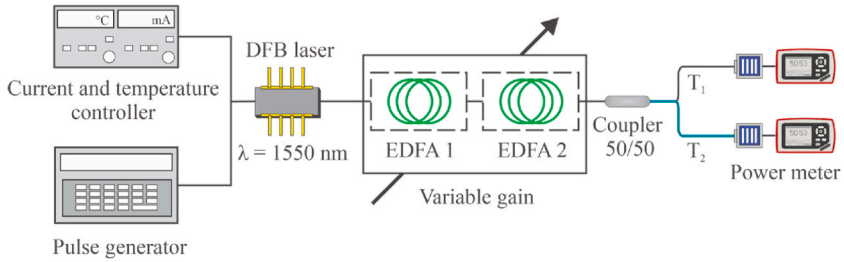

Fig. 4. Experimental setup for measurement of the saturable absorption properties of the GOQDs.

deconvolution of these two bands showed two additional bands at 1350 cm^{-1} (D*) and at 1608 cm^{-1} (D''), associated with lattice vibrations corresponding to sp^2 and sp^3 hybridizations and the distribution of impurities in interstitial network sites, respectively [27].

After the exfoliation process of the carbonized fibers, TEM analysis confirmed the quasi-spherical morphology of the obtained GOQDs, with an average size of 6 nm, as shown in the right top inset in Fig. 2a. The left bottom inset shows the micrograph of a GOQD whose calculated interplanar distance was 0.19 nm, corresponding to the direction (002) of graphene oxide (JCPDS Card No. 75–1621) [28].

The FTIR spectrum of the GOQDs is shown in Fig. 2b, where absorption signals are observed in the region from 3020 to 2820 cm-1 associated with the aliphatic groups CH (CH, CH2 and CH3), as well as vibrations in the region of 1750 cm-1 associated with C═O bonds, the signals in the region from 1380 to 1350 cm-1 belonging to the stretching vibrations of the C═O bonds [29].

Fig. 2c shows the Raman spectrum of the GOQDs, where the D (1312 cm-1) and G (1583 cm-1) bands related to graphene oxide [30] are observed. The intensity of these bands allows us to predict the existence of a restructuring of the carbon atoms in the GOQDs to a sp2 hybridization, associating an increase in the concentration of electrons in the GOQDs [31]. The change of intensities on D and G bands indicates that the crystal lattice of the GOQDs presents a higher order with fewer defects or impurities compared to the carbonized fibers, as observed in Fig. 2c.

2.3. 2.3 Photodeposition and nonlinear characterization of GOQDs

The photodeposition of the GOQDs on the optical fiber was carried out using the technique reported by Ortega-Mendoza et al. [32, 33], using a continuous wave laser (THORLABS model FPL1009S) with a wavelength of 1550 nm. This technique consists of removing

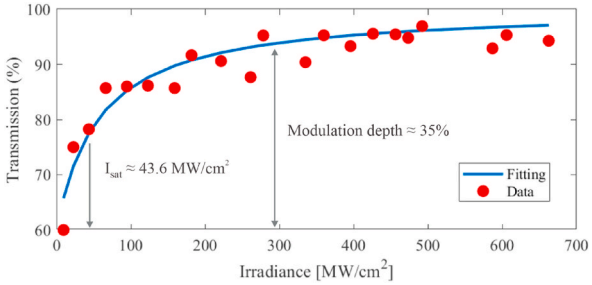

Fig. 5. Nonlinear transmission curve of the GOQDs photodeposited onto the optical fiber.

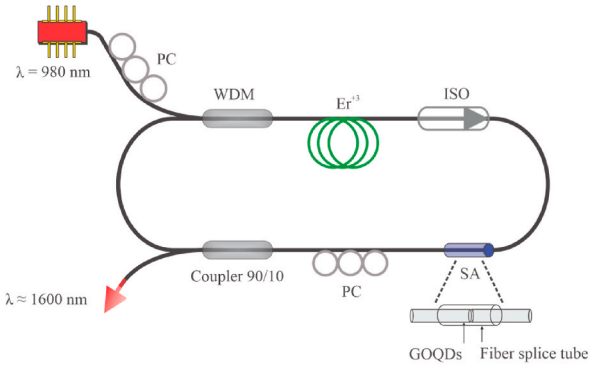

Fig. 6. Experimental setup for fiber pulsed laser using GOQDs as SA.

the plastic coating from a single-mode optical fiber (SMF-28+) and making a transverse cut using a fiber stripper to subsequently introduce the tip of the optical fiber into the solution, as is shown in Fig. 3. The colloidal solution was prepared by mixing 2.3 mg of GOQDs in 1 ml of isopropyl alcohol. The photodeposition was carried out by immersing the optical fiber in the colloidal solution until a power loss of 1.25 dB was obtained, which was verified using a power meter (THORLABS model PM100D) and an integrating sphere power sensor (THORLABS model S145C).

Nonlinear characterization was performed using the P-scan technique with a high-gain EDFA [34]. The array consisted of an optical signal emitted by a distributed feedback (DFB) laser with emission at 1550 nm. The signal was controlled by a pulse generator (BNC model 6040) and stabilized with a temperature/current controller. The array was configured to obtain a pulsed emission at a frequency of 1 kHz and a time width of 20 ns; under these conditions, it was possible to obtain a maximum irradiance of 650 MW/cm2. A 50/50 coupler was placed at the terminal of the EDFA to carry out the transmission analysis as shown in Fig. 4. The signal at terminal T1 was used as reference (input signal), while terminal T2 was used as device under test (output signal).

The nonlinear transmission study of the photodeposited GOQDs was carried out using the Beer-Lambert law [35,36], which describes the absorption of laser radiation in a substrate, expressed as:

$$T = exp[-\alpha(I)L], \tag{1}$$

where α(I) is the absorption coefficient, I is the incident intensity, and L is the thickness of the sample. The absorption coefficient can be expressed as a function of the linear (α_0) and non-linear absorption coefficients of the material (β), resulting in the following expression:

$$T = exp[-(\alpha_0 + \beta I)L]. \tag{2}$$

The experimental results of the NLC of the GOQDs photodeposited in the core of an optical fiber are shown in Fig. 5. The dots correspond to the experimental measurements and the solid line corresponds to the fit using Eq. (2) with an I_{sat} = 43.6 MW/cm^2, obtained from the experimental data using a hyperbolic approximation model. Under these conditions, it was possible to determine the values of the non-linear absorption coefficient $\beta = -1.178\,x10^{-6}$ (m/W) and non-linear susceptibility $Im(\chi^{(3)}) \approx -1.573x10^{-7}$ (esu), respectively. Recent studies have demonstrated that the modulation depth can be adjusted through the quantity of photodeposited nanostructures on the fiber core, as indicated by the reports presented by Cuvas-Limón et al. [37] and Gómez-Pavón et al. [38]. These studies show that an increase in modulation depth is directly related to an increase in radiation transmission losses during the photodeposition process. In other words, by increasing the volumetric amount of photodeposited GOQDs in the fiber core during the photodeposition process, a greater modulation depth can be achieved. It is important to mention that during the NLC of GOQDs, it was observed that the transmission increases during each measurement by approximately 5%. This behavior causes a proportional

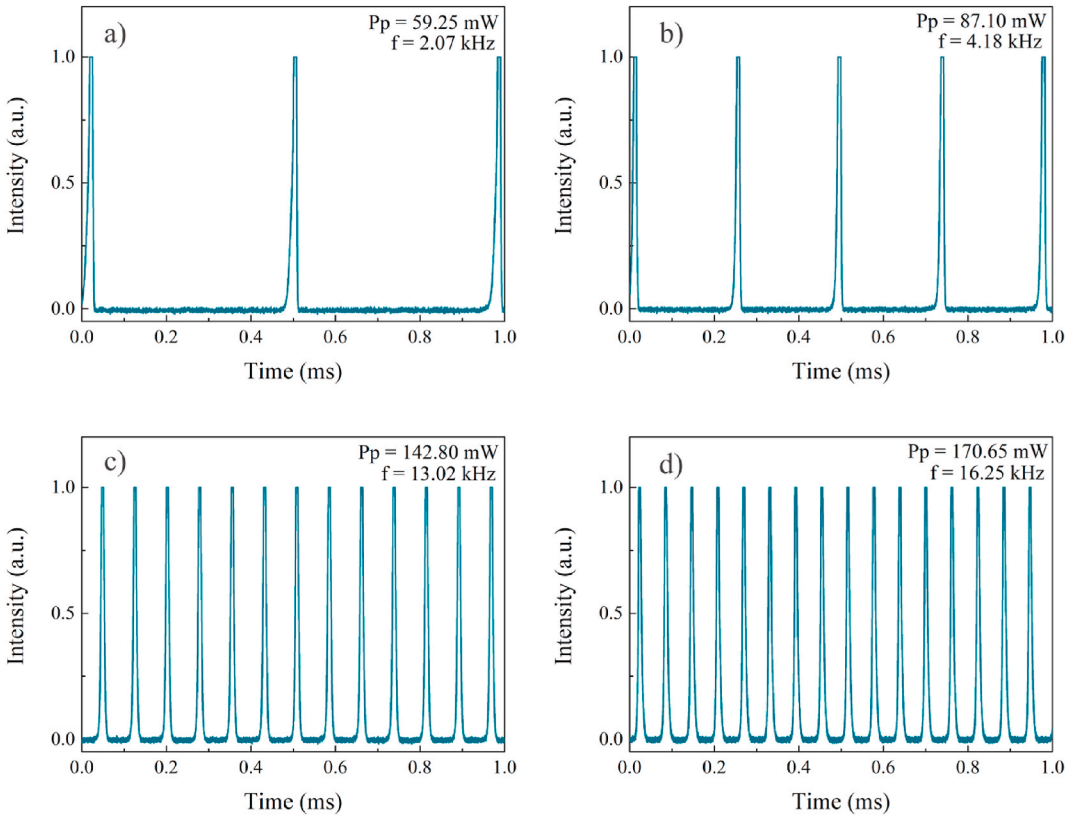

Fig. 7. Traces of Q-switched laser output pulse train at different pump powers: a) 59.25, b) 87.10, c) 142.80, and d) 170.65 mW, respectively.

reduction in the depth of modulation. We think that the radiation pressure generated by the pulsed signal causes detachment of the GOQDs located onto the fiber core, resulting in more radiation passing through its core.

2.4. Q-switched fiber laser

The experimental arrangement of the optical fiber laser using a ring cavity configuration is shown in Fig. 6. An erbium-doped fiber was used as the gain medium and a laser diode with a wavelength of 980 nm was used as pumping mechanism through a wavelength division multiplexer (WDM). An optical isolator (ISO) was inserted into the cavity to guarantee unidirectional operation of the laser and a polarization controller (PC) has been incorporated to adjust and optimize the polarization circulating in the cavity, thereby enhancing the laser's output power emission. A 90/10 directional coupler was placed to extract 10% radiation and 90% feedback into the cavity.

The optical fiber with the GOQDs was inserted into the cavity as a switching device, which was connected through a ~150 μm diameter borosilicate glass capillary tube. Spectral characteristics of the output of the laser were observed in an optical spectrum analyzer (Anritsu model MS9740A) at a resolution of 0.1 nm and the frequency emission was characterized using a photodiode (THORLABS model DET01CFC) and an oscilloscope (Tektronix model TDS 3054C).

3. Experimental results and discussions

Experimental results showed that pulsed laser emission was possible using GOQDs as a SA, which was activated at a threshold power of 60 mW (the power at which it starts to behave like a laser); however, the pulses were able to stabilize for a few minutes. To stabilize the emission inside the cavity, isopropyl alcohol was added in the capillary tube, thus allowing stable laser emission. Under these conditions, the results obtained from the pulsed emission showed an adjustable pulse repetition rate from 2 to 16 kHz by varying the pump power from 59.2 to 170 mW. Fig. 7 (a - d) shows the oscillograms of the pulsed laser for different pump powers of 59.25, 87.10, 142.80, and 170.65 mW, respectively.

Fig. 8 shows the dependence of the pulse frequency and width as a function of the pump power. According to the results obtained, a stable pulsed emission was observed for a range of pump powers between 60 and 170 mW. In Fig. 8a is shown that for a pump power of 60 mW, the laser emits a pulse with a duration of 12 μs and a frequency of 2 kHz; subsequently, as the pump power increases, the pulse width decreases, which is a typical behavior of a Q-switched laser. Fig. 8b shows the average output power of the pulses as a function of

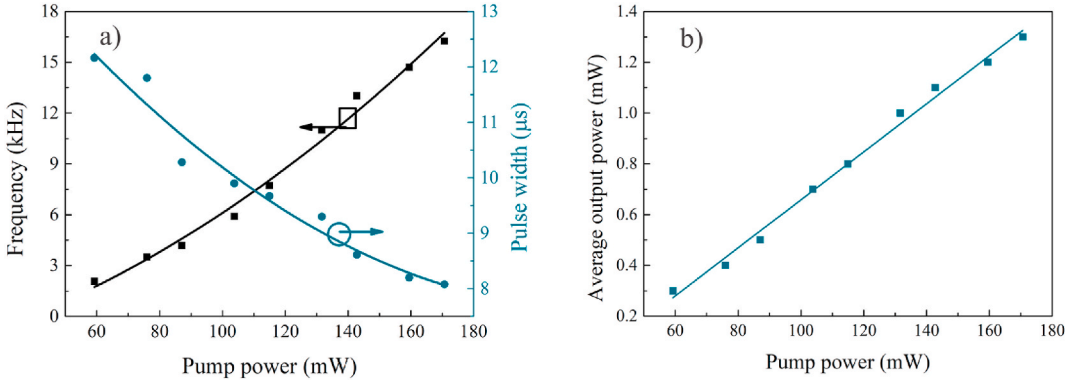

Fig. 8. a) Frequency and pulse width as a function of the incident pump power, and b) Output power as a function of pump power.

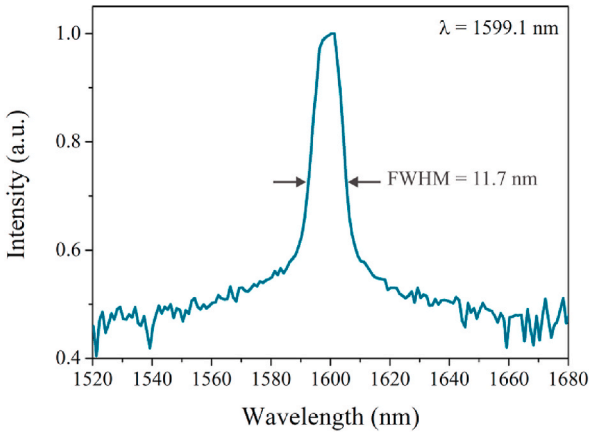

Fig. 9. Optical spectrum of the output pulse of Q-switched fiber laser.

the pump power, which is between 0.3 mW for the lowest power and 1.3 mW for the highest power. In addition, the output emission spectrum of the laser is shown in Fig. 9, which shows emission at a wavelength of 1599.1 nm and a Full Width at Half Maximum (FWHM) of 11.7 nm.

In this study, GOQDs were fabricated from a polymeric material and used as a saturable absorption device in an optical fiber laser. The fabricated GOQDs showed optical properties like semiconductor crystals, intense fluorescence, and non-toxic nature, rendering them suitable for nonlinear optics applications. The laser operates in a Q-switched state, with a lower pump threshold using GOQDs photodeposited onto the end of an optical fiber, into the laser cavity as a saturable absorber. The SA presented here works stably with repeatable operation settings. This saturable absorber is very attractive for applications such as pedestal suppression and amplitude regulation of optical signals, optical switching, and passive mode-locking. Recent studies have emphasized the potential of GOQDs not only to enhance light modulation and manipulation, but also as promising candidates across diverse realms of photonics and opto-electronics. Their contribution to advancements in these fields has fostered innovation in technological developments and practical applications [39]. To our knowledge, this is the first report of an optical fiber laser based on graphene oxide quantum dots used as a passive switching device.

4. Conclusions

In this work, the pulsed emission of a Q-switched laser using GOQDs photodeposited on an optical fiber as switching device was shown. The GOQDs were obtained from the carbonization and exfoliation of PAN electrospun fibers, whose nonlinear properties showed a saturable absorption behavior. The Q-switched laser emitted short pulses between 8 and 12 μs at a tunable repetition frequency from 2 to 16 kHz. Although the optical fiber with photodeposited GOQDs can generate optical pulsed emission inside the cavity for short periods of time, it was necessary to add isopropyl alcohol inside the capillary tube to stabilize the pulse indefinitely. Our experimental results clearly demonstrated that GOQDs can be considered a suitable candidate for application in a Q-switched laser, with potential application in switching devices.

Author contribution statement

P. Zaca-Morán: Conceived and designed the experiments; Analyzed and interpreted the data; Wrote the paper.
Celia L. Gomez: Analyzed and interpreted the data; Contributed reagents, materials, analysis tools or data; Wrote the paper.
O. Zaca Morán: Conceived and designed the experiments; Performed the experiments; Contributed reagents, materials, analysis tools or data.
J. G. Ortega-Mendoza: Analyzed and interpreted the data; Contributed reagents, materials, analysis tools or data.
E.S. Pola-López: Conceived and designed the experiments; Performed the experiments; Analyzed and interpreted the data.

Data availability statement

Data will be made available on request.

Declaration of competing interest

The authors declare that they have no known competing financial interests or personal relationships that could have appeared to influence the work reported in this paper.

Acknowledgments

The research leading to these results has received funding from the BUAP, through the Vice-president for Research and Post-graduate Studies and the Science Institute (ICUAP) under grant agreement no. 365/2022 also, from the Instituto Politecnico Nacional trough the SIP project 20231709. Project supported by CONAHCYT in 2023 (CF-2023-G-1080) and under grant agreement no. BP-PAIM-20220906151734769-3682852.

References

[1] Z. Liu, et al., Nonlinear optical properties of graphene-based materials, Chin. Sci. Bull. 57 (23) (2012) 2971–2982.
[2] C.-H. Cheng, G.-R. Lin, Carbon nanomaterials based saturable absorbers for ultrafast passive mode-locking of fiber lasers, Curr. Nanosci. 16 (3) (2020) 441–457.
[3] D. Stoliarov, et al., Saturable absorber based on the fiber coupler coated by CNTs, Opt. Fiber Technol. 63 (2021), 102524.
[4] J. Zou, et al., Visible-wavelength pulsed lasers with low-dimensional saturable absorbers, Nanophotonics 9 (8) (2020) 2273–2294.
[5] X. Peng, Y. Yan, Graphene saturable absorbers applications in fiber lasers, J. Eur. Opt. Soc. Rapid Publ. 17 (1) (2021) 1–26.
[6] Y. Wang, et al., Passively mode-locked solid-state laser with absorption tunable graphene saturable absorber mirror, J. Lightwave Technol. 37 (13) (2019) 2927–2931.
[7] M. Hussain, et al., Effects of flake size on mode-locking behavior for flake-graphene saturable absorber mirrors, Optik 198 (2019), 163232.
[8] R. Zhang, et al., Tunable Q-switched fiber laser based on a graphene saturable absorber without additional tuning element, IEEE Photon. J. 11 (1) (2019) 1–10.
[9] X. Zhu, S. Chen, Study of a graphene saturable absorber film fabricated by the optical deposition method, IEEE Photon. J. 11 (6) (2019) 1–9.
[10] J. Wang, et al., Nonlinear optical response of graphene oxide Langmuir-blodgett film as saturable absorbers, Nanomaterials 9 (4) (2019) 640.
[11] G. Zhang, et al., Graphene oxide based reflective saturable absorber for Q-switched and mode-locked YVO4/Nd: YVO4/YVO4 laser, J. Opt. 20 (5) (2018), 055505.
[12] L. Hou, et al., High-efficiency, high-energy ytterbium-doped Q-switched fibre laser with graphene oxide-COOH saturable absorber, Laser Phys. Lett. 15 (7) (2018), 075103.
[13] N. Kasim, et al., Short-pulsed Q-switched Thulium doped fiber laser with graphene oxide as a saturable absorber, Optik 168 (2018) 462–466.
[14] Y. Yap, et al., Performance of Q-switched fiber laser using optically deposited reduced graphene oxide as saturable absorber, Fiber Integr. Optics (2022) 1–15.
[15] E. Ng, et al., Saturable absorber incorporating graphene oxide polymer composite through dip coating for mode-locked fiber laser, Opt. Mater. 100 (2020), 109619.
[16] J. Chang, et al., Efficient and compact Q-switched green laser using graphene oxide as saturable absorber, Opt Laser. Technol. 98 (2018) 134–138.
[17] Y.-K. Yap, et al., Simple fabrication of paper-like graphene oxide for use as saturable absorber in q-switching of fiber laser, J. Appl. Sci. Eng. 24 (4) (2021) 509–516.
[18] S. Liu, et al., Two-photon saturable absorption properties and laser Q-switch application of carbon quantum dots, Opt Lett. 42 (19) (2017) 3972–3975.
[19] N. Radzi, et al., Q-switched fiber laser based on CdS quantum dots as a saturable absorber, Results Phys. 16 (2020), 103123.
[20] S. Ahmed, et al., Tin telluride quantum dots as a novel saturable absorber for Q-switching and mode locking in fiber lasers, Adv. Opt. Mater. 9 (6) (2021), 2001821.
[21] Y.-W. Lee, et al., Passively Q-switched Er 3+-doped fiber lasers using colloidal PbS quantum dot saturable absorber, Opt Express 24 (10) (2016) 10675–10681.
[22] L. Dong, et al., Passively Q-switched near-infrared lasers with bismuthene quantum dots as the saturable absorber, Opt Laser. Technol. 128 (2020), 106219.
[23] N. Xu, Q. Wen, Single element material sulfur quantum dots nonlinear optics and ultrafast photonic applications, Opt Laser. Technol. 138 (2021), 106858.
[24] O. Zaca-Moran, et al., Electrospun polyacrylonitrile nanofibers as graphene oxide quantum dot precursors with improved photoluminescent properties, Mater. Sci. Semicond. Process. 127 (2021), 105729.
[25] M.A. Hossain, S. Islam, Synthesis of carbon nanoparticles from kerosene and their characterization by SEM/EDX, XRD and FTIR, Am. J. Nanosci. Nanotechnol. 1 (2) (2013) 52.
[26] M. Dresselhaus, et al., Defect characterization in graphene and carbon nanotubes using Raman spectroscopy, Phil. Trans. Math. Phys. Eng. Sci. 368 (1932) (2010) 5355–5377.
[27] S. Claramunt, et al., The importance of interbands on the interpretation of the Raman spectrum of graphene oxide, J. Phys. Chem. C 119 (18) (2015) 10123–10129.
[28] M. Tuerhong, X. Yang, Y. Xue-Bo, Review on carbon dots and their applications, Chin. J. Anal. Chem. 45 (1) (2017) 139–150.
[29] O. Sadak, A.K. Sundramoorthy, S. Gunasekaran, Facile and green synthesis of highly conducting graphene paper, Carbon 138 (2018) 108–117.
[30] R. Saito, et al., Double resonance Raman spectroscopy of single-wall carbon nanotubes, New J. Phys. 5 (1) (2003) 157.
[31] A. Mikhraliieva, et al., Graphene oxide quantum dots immobilized on mesoporous silica: preparation, characterization and electroanalytical application, RSC Adv. 10 (52) (2020) 31305–31315.
[32] J. Ortega-Mendoza, et al., Selective photodeposition of zinc nanoparticles on the core of a single-mode optical fiber, Opt Express 21 (5) (2013) 6509–6518.

[33] P. Zaca-Morán, et al., Saturable and two-photon absorption in zinc nanoparticles photodeposited onto the core of an optical fiber, Opt Express 23 (14) (2015) 18721–18729.
[34] P. Zaca-Morán, et al., High gain pulsed erbium-doped fiber amplifier for the nonlinear characterization of SWCNTs photodeposited on optical fibers, Opt Laser. Technol. 52 (2013) 15–20.
[35] W. Steen, J. Mazumder, K. Watkins, Laser Material Processing, Springer, 2010, 2008.
[36] N. Roy, A. Kuar, S. Mitra, Underwater pulsed laser beam cutting with a case study, in: Microfabrication and Precision Engineering, Elsevier, 2017, pp. 189–212.
[37] J.M. Cuvas-Limón, et al., Measurement of two-photon absorption by gold nanoparticles of different sizes photodeposited onto the core of an optical fibre, Lith. J. Phys. 61 (1) (2021).
[38] L. Gómez-Pavón, et al., Influence on the saturable absorption of the induced losses by photodeposition of zinc nanoparticles in an optical fiber, Opt Express 26 (2) (2018) 1556–1563.
[39] K. Zhang, et al., Concentration modulated photoluminescence and optical switching performance of graphene-oxide quantum dots, J. Lumin. 209 (2019) 116–120.